Solid State Phenomena
ISSN: 1662-9779, Vol. 389, pp 107-114
doi:10.4028/p-Odegn2

Submitted: 2025-12-22
Revised: 2026-02-18
Accepted: 2026-02-24
Online: 2026-04-16

Pressure Wave Analysis in Electrohydraulic Forming – A Multiple Sensor Approach

Lasse LANGSTÄDTLER[1,2,3,a*], Andreas TAUSENDFREUND[1,2,4,c] and Christian SCHENCK[1,2,3,b]

[1]University of Bremen, Bibliothekstraße 1, 28359 Bremen, Germany

[2]MAPEX - Center for Materials and Processes, 28334 Bremen, Germany

[3]Bremen Institute for Mechanical Engineering, Badgasteiner Straße 1, 28359 Bremen, Germany

[4]Bremen Institute for Metrology, Automation and Quality Science, Linzer Strasse 13, 28359 Bremen, Germany

[a*]lasse.langstaedtler@uni-bremen.de, [b]cschenck@uni-bremen.de, [c]a.tausendfreund@bimaq.de

Keywords: Electrohydraulic forming, pressure wave, shockwave, schlieren imaging

Abstract. Electrohydraulic forming involves a complex energy transfer from the initial plasma explosion through the fluid to the sheet metal, where the pressure wave propagation critically determines the amplitude, distribution, and timing of the resulting acceleration forces. These dynamics can be influenced not only by the explosion itself but also by fluid properties and the geometry and volume of the pressure vessel. To enable systematic process optimization, this study introduced a multi-sensor methodology that captured the transient behavior of the forming process. The approach integrated piezoelectric pressure sensor measurement and high-speed background-oriented schlieren imaging to analyze the pressure wave propagation, as well as in-situ two-point laser triangulation to monitor the sheet metal displacement. Experiments using different exploding wires varying discharge energies demonstrate the method's effectiveness. The results reveal different pressure wave velocities from 800 m/s to 1700 m/s and link displacement data to wave-induced impulses. Additional phenomena such as process-related light emissions and cavitation bubble formation were temporally resolved. The study further introduced that, after an initial learning phase with full sensor integration, selected sensors can be omitted in specific scenarios without loss of essential information, highlighting the efficiency and adaptability of the proposed diagnostic approach.

Introduction

In the manufacturing of parts with complex channel structures, media-based high-velocity forming processes such as wire based electrohydraulic forming offer significant advantages in terms of contactless force transmission and reduced spring back.

Impulse forming processes have been introduced to thin sheet metal forming and micro production in recent years [1]. The investigations showed advantages regarding flexibility in tooling, material behavior like spring back calibration as well as energy efficiency [2]. When applied to bipolar plates, these benefits translate into higher efficiency and with reduced component weight. However, due to the complex interactions among multiple physical domains such as electromagnetics, structural mechanics, and fluid dynamics, as well as governing pressure generation, propagation within the fluid, and the forming of the component, an accurate description and design of media-based impulse forming processes is not yet feasible. [3]

Different investigations were conducted to analyze the multi physical aspects starting from the pressure wave generation. In the near-field, the plasma channel behavior showed a correlation to the discharge current and wire properties which finally influenced the effectiveness of the propagation pressure wave due to peak pressures [4]. The wave speed was determined to be lower in the near-field than in the far-field [5]. In the far-field, the speed of sound is expected to be the wave velocity

in electrohydraulic forming. Thus, it can be assumed that the shockwave speed is influenced by the fluid pressure [6].
The mapping of pressure fields by forming results was shown by Eguia et al. [7]. They described gradients in the electrohydraulic forming results that were related to the transient pressure action which could be reduced using exploding wires. To generate a real insight into the process, in-situ two-point laser triangulation of the sheet metal displacement was introduced to electrohydraulic forming [8]. There are various publications on the simulation of pressure wave propagation in electrohydraulic forming [9]. However, there is no coherent analysis, and the pressure wave in the fluid as a mode of transmission has not yet been experimentally proven for electrohydraulic forming. The presented research focused on developing a multi-sensor approach for electrohydraulic forming. Consequently, the main aim was to prove this approach by a first fundamental analysis of the interactions between adjustable process parameters, the transient pressure field within the working fluid and the forming process for electrohydraulic forming. Therefore, in the first step the pressure wave was investigated. The aim was to detect the pressure wave based on the different sensors as it was assumed to be a main influencing factor to understand the energy transmission in the working media process. The pressure wave was then described by wave speed, amplitude and curvature within the pressure vessel. With a view toward potential application in bipolar plates, the investigations focused on 1.4404 sheet material with a thickness of 0.1 mm and wire based electrohydraulic forming.

Materials and Methods

Testing set-up and procedure. A pulsed-power machine was used for electrohydraulic forming, Figure 1a. The pulsed-power machine consisted of a capacitor bank (8x E62.S24-503C60, electronicon GmbH, Gera, Germany) with a capacitance of C = 100 µF which was loaded by a high-voltage power supply (HPP120656-CLD, iseg GmbH, Radeberg, Germany) to the loading voltage U_0. The capacitor bank was short-circuited by a high current switch (ignitron NL8900, National Electronics, LaFox, Il, USA) over a wire with 20 mm length. Consequently, a peak current arose which vaporized the wire resulting in a wire plasma explosion. The wire was attached between two insulated electrodes placed in a pressure chamber stacked with further functional rings - pressure ring, inspection window ring - and the forming die. The resulting pressure vessel was filled with distilled water as a pressure transmitting working media, Figure 1b. This approach integrated piezoelectric pressure sensor measurement and high-speed background-oriented schlieren (BOS) imaging to analyze the pressure wave propagation as well as in-situ two-point laser triangulation to monitor the sheet metal displacement which also can be related to the energy transfer according to the pressure wave.

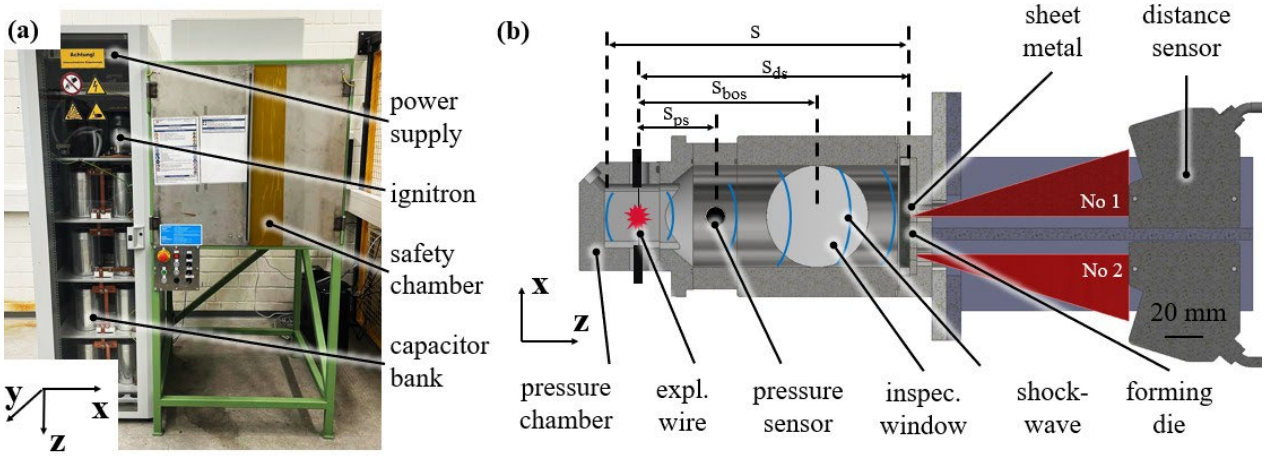

Fig. 1. Testing set-up: (a) pulsed-power machine, (b) cross-sectional view of pressure chamber assembly

Two different set-ups A and B with different heights s and same 70 mm diameter of the pressure vessel - with and without inspection window ring - were used in this work for different testing scenarios, table 1. The annealed stainless-steel sheet (EN 1.4404 / AISI 316L) with dimensions of 100×100 mm² and a thickness s_0 of 100 µm was placed on the forming die.

Table 1. Testing scenarios

scenario	set-up	pressure vessel height s [mm]	sensors	loading energy [J]	wires
1	A	210	pressure, schlieren, displacement	50, 68, 85	Cu99: d = 0.28 mm, R = 1.63
2	B	100	pressure, displacement	85	Al99.5: d = 0.35 mm, R = 1.49 Cu99: d = 0.28 mm, R = 1.63 W99: d = 0.18 mm, R = 1.93

A round blank holder with a diameter of 70 mm was used. O-rings were applied between pressure chamber and rings as well as face plate and sheet metal. The pressure waves of the wire explosion traveled through the water and caused pressure on the sheet metal. The sheet metal was consequently formed on a milled die made of EN 1.4301 / AISI 304. The whole forming package was mounted in a clamping frame.

In testing scenario 1, the loading energy E_C was varied from 50 J to 85 J. The tests were performed with 0.28 mm pure copper wire resulting in a quotient R (cp. Eq. 1 [8]) of the loading energy and the vaporization energy E_V - according to the volume V, the density ρ and the vaporization enthalpy Δh_v of the wire - from R ≈ 1 to R = 1.6. It was assumed that the wire evaporated differently by variation of the supplied energy which resulted in changes in the pressure wave propagation and forming. Here, it should be noted that the additional melting energy required was assumed to be negligible. In this scenario the distance between wire axis and sheet metal was 184 mm.

$$R = \frac{E_C}{E_V} = \frac{0.5 \cdot C \cdot U_0^2}{V \cdot \rho \cdot \Delta h_v} \quad (1)$$

In testing scenario 2, the wires were varied using pure aluminium (Al99.5), pure copper (Cu99) and pure tungsten (W99) whereas the loading energy was kept constant with E_c = 85 J. In this scenario the distance between wire axis and sheet metal was reduced to 74 mm.

A free-forming die was used which enabled two simultaneous bulging operations by rectangular cut-outs of 8×16 mm² with 3 mm edge radius. The workpiece was held down with a gap of 0 mm to the die. All tests were repeated three times.

Measurement set-up and procedure. The multi-sensor methodology was used to analyze the transient behavior of the forming process. The measuring equipment and USB oscilloscope used were operated using a separate potential-free power supply, and the measuring computer was used in battery mode. Based on the two different test scenarios, different sensors were considered in the wave analysis.

A piezo-electric pressure sensor (102B03, PCB piezotronics GmbH, Hückelhoven, Germany) was used with a battery powered signal conditioner (480C02, PCB piezotronics GmbH, Hückelhoven, Germany). The pressure sensor was mounted uninsulated in the pressure ring with s_{ps} = 64 mm. Triggered by the discharge current which coupled into the measurement signal as interference, the pressure sensor time period Δt_{ps} to the first pressure peak could be determined which was in the range of around 100 microseconds, Fig. 2a. The peak was chosen since following peaks could be used for reflection analysis in future. The time was correlated to the distance from wire to pressure sensor and assumed to represent the formation of the pressure wave from near- to far-field to a certain mean value of pressure wave velocity v_{ps}.

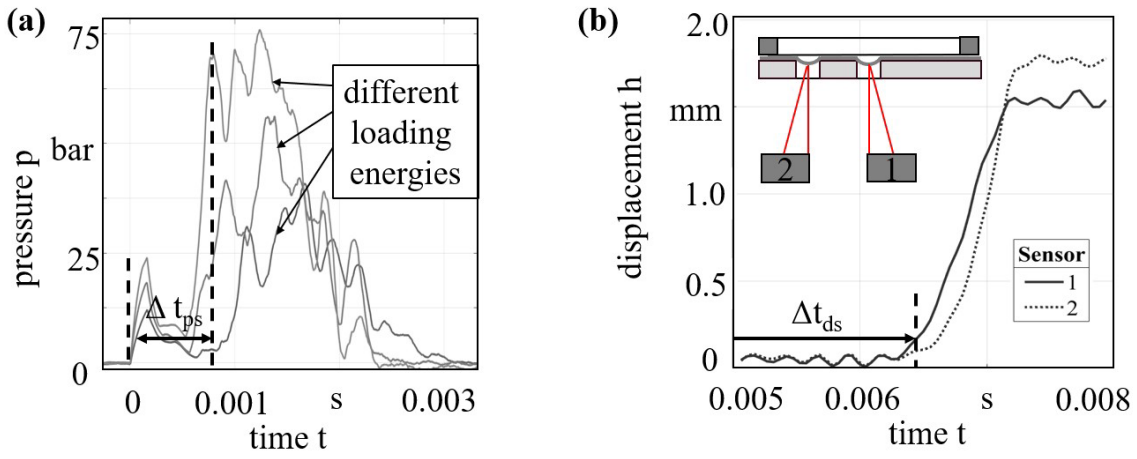

Fig.2. Measurement: (a) example pressure curves for different loading energies 100 J - 400 J, (b) example measured displacement h as a function of time t [8]

The sapphire inspection window (diameter of Ø80 mm and thickness of 20 mm) gave access to the fluid chamber for schlieren imaging. The high-speed camera (fastcam nova S12, photron, Reutingen, Germany) enabled recording rates of 200,000 fps which resulted in shutter speeds of Δt_{bos} = 5 µs. To realize the background oriented schlieren method, a speckle pattern with speckle size of around 1 mm and distance of around 3 mm was placed on the backside of the fluid reservoir on a second inspection window. This second window enabled sufficient background lighting by a power LED. Triggering the collection of video frames by the process lightning, the pressure wave travels along the inspection window - with the center at s_{bos}= 122 mm to the wire axis. The pressure wave could be seen by differential imaging (Fig. 3a) and by BOS-imaging with cross-correlation code using matlab [9], Fig. 3b. The transient frame by frame information of speed v_{bos_f} can be calculated by the quotient of travelled pixels and the distance Δs_{bos} and Δt_{bos}. Furthermore, two kind of mean value velocities v_{bos_m} were calculated. One value was based on the distance from wire to the center of the window and the time period starting from process lighting. The second value was calculated based on the local velocities from frame to frame.

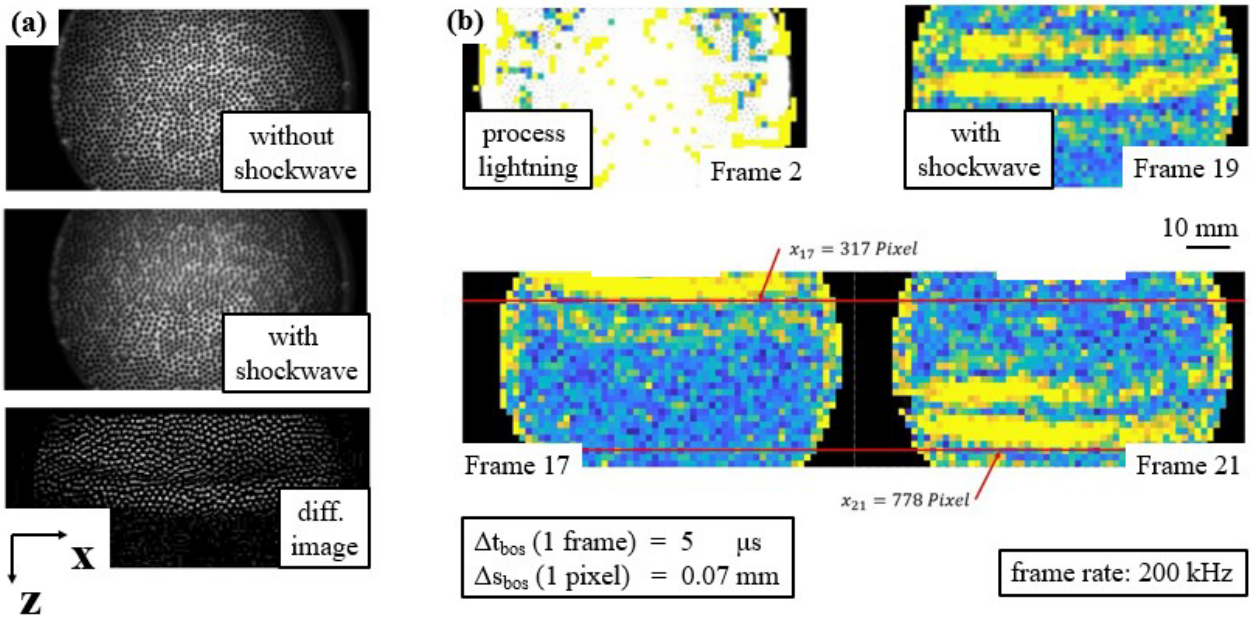

Fig. 3. Measurement: (a) raw view through inspection window and differential image, (b) cross-correlated images and visualization of pressure wave

Two photoelectric sensors (LK-H157, Keyence, Osaka, Japan) were implemented for in-situ measuring the displacement h of the workpiece in the center (sensor 1) and 26 mm to the side (sensor

2) sampled every 2.55 µs, Fig. 2b. This arrangement enabled a two-point insight into the arising pressure field. The measurement set-up was operated with a separate electrical potential (hv-disconnected) to reduce electrical interferences. The distance between sheet metal and wire axis depended on the testing scenario s_{bos} = 184 mm and 74 mm. The time period Δt_{ds} was then determined by calculation for a 5 % threshold value of the maximum sheet metal velocity. This time period was in the range of a few hundred microseconds.

Results

The pressure sensor data provided insight into the area between the wire and the pressure sensor. This area could also be described as the near-field. The time to maximum pressure decreased, resulting in a slight increase in wave velocity from 830 to 870 m/s for different loading energy values, Figure 4a. Furthermore, the choice of wire material at a constant charging energy of 85 J had a significant influence on the wave velocity calculated using pressure sensor data. The highest wave velocities in the near field were calculated for copper wire, followed by aluminum and tungsten, Figure 4b.
With increasing propagation, the wave became visible and measurable in the inspection window area. Here, the wave travelled into the far-field region. The BOS-data was collected in test scenario 1. The velocity of the wave was determined in different variants. Figure 5a shows the average velocity over five frames and the average over the time from the process lightning to detection in the inspection window. Here too, in both cases the wave velocity increased with the loading energy. At the same time, the two calculation variants led to slightly different values. What must be highlighted here is, the waves were identified as shock waves with velocities of 1650 m/s to 1720 m/s. For the energy variation the shock waves showed a comparable curvature.

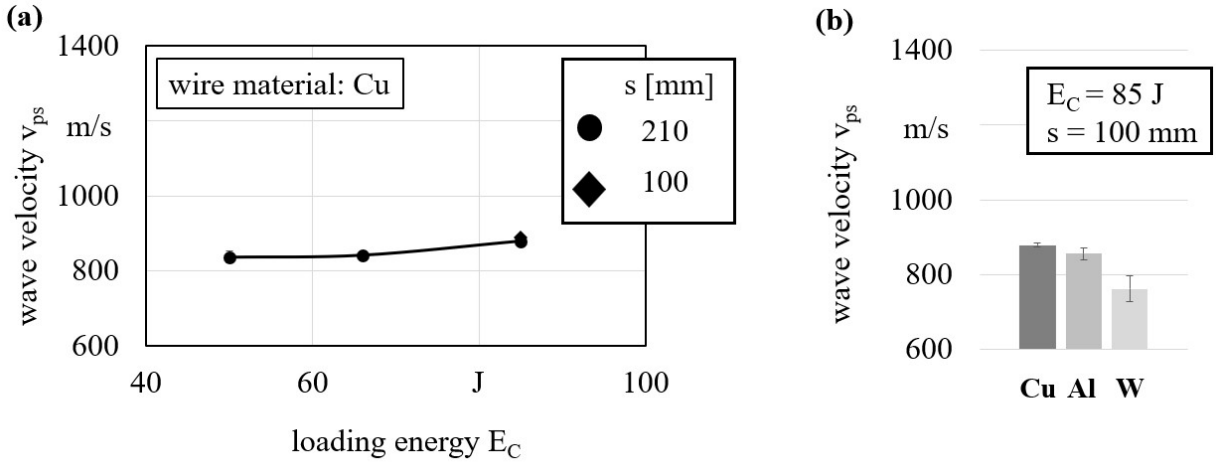

Fig. 4. Pressure sensor data: (a) calculated wave velocity as a function of the loading energy, (b) wave velocity for different wire materials

In all cases clear main wave fronts were detected and used for determination of the velocities, however, for higher energies an increase of reflection appeared. Regarding the wave velocity along the inspection window, it was determined to be constant for the lowest charging energy. With increasing charging energy, there was an increase in wave velocity up to 1800 m/s from frame to frame, Fig. 5b. Nevertheless, this transient wave velocity within a few microseconds could also be attributed to measurement uncertainties.

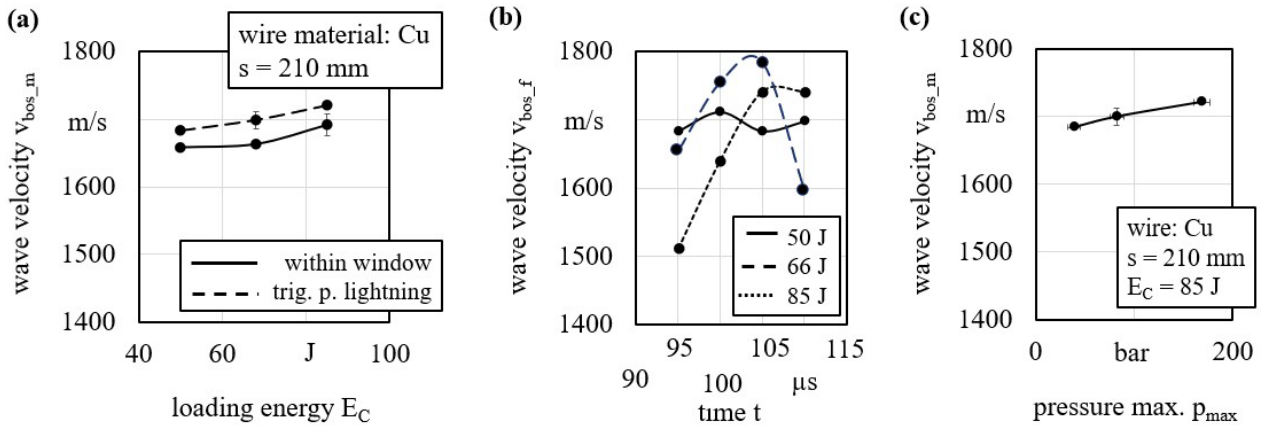

Fig.5. BOS Method data: (a) average wave velocity as a function of the loading energy, (b) wave velocity as a function of time, (c) correlation of maximum pressure value and wave velocity

As the wave continued to move forward, it reached the sheet metal and caused a free forming. The calculated wave velocity was determined to increase with the loading energy from 800 m/s and then reached a maximum value of around 1300 m/s, Fig. 6a. At the same time, there were differences in the values obtained when using sensors 1 and 2 of 10 %, which can be attributed to the curvature of the wave. Compared to the pressure sensor and the BOS method, this variant led to higher fluctuations in the calculated velocities. In addition, lower velocities were determined for the set-up with smaller pressure vessel height s, whereas the difference between sensor 1 and 2 occurred again. Wave velocities for different wire materials were calculated to be constant, Fig. 6b.

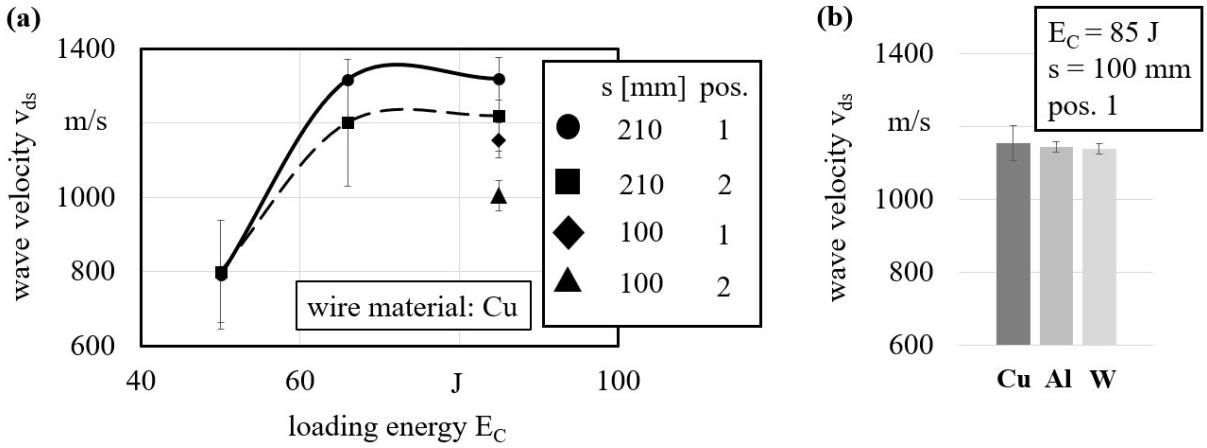

Fig. 6. Distance sensor data: (a) wave velocity as a function of the loading energy, (b) wave velocity at sensor 1 for different wire materials

Discussion

The velocity of the pressure wave could be calculated based on different sensor data. However, differences in the velocities accrued that could be referred to physical effects and the pressure wave propagation as well as the determination of distances and time periods Δt_i.

For the pressure sensor there were two influencing factors to be critically discussed - the start trigger and stop trigger. As start trigger the current peak was used. However, it could be expected that there was a time difference between the electrical discharge, the wire explosion and the breaking away of the pressure wave. Hence, the velocity was underestimated. The pressure peak was used as end trigger. Here, the wave event theoretically begins shortly beforehand with the rising pressure value, which again leads to an underestimation of the velocity. Nevertheless, it was assumed that this error in the range of 10% does not change the fact that the pressure sensor-based velocities are the lowest. This was explained by the non-linearity of the explosion and wave propagation in the near-field.

Although it required more effort to use, the BOS-method provided a detailed view into the pressure vessel fluid. This allowed various phenomena to be observed directly – not only detecting the shockwaves presence and velocity, but also its geometry and process lighting as well as the occurrence of gas bubbles. The theoretical error that appeared when selecting the start trigger for calculating an average velocity could be prevented by evaluating the velocities within the inspection window. The only error that remained to be mentioned here was caused by the resolution of the camera which was reduced at high frame rates. However, this error was very low according to the resolution of 0.07 mm per pixel.
Considering the BOS- data - even though this observation was confirmed in the other data - an increase in velocity was observed by increasing loading energy. In the case of pressure and distance sensor data this could be again explained by an error in time period calculation. However, this behavior was confirmed as valid using the BOS-method and can be explained by the increasing pressure in the fluid which has an influence on the speed of sound, cp. Fig. 5c. Similarly, this explained why a value higher than theoretical velocity at atmosphere pressure was measured even at the lowest energy level.
The distance sensor data reacted more sensitively to variations in the charging energy. This could be attributed to errors in the start trigger regarding the discharge current and the calculation of the end trigger which may be affected by delay due to sheet metal inertia. Nevertheless, the two sensors provided further information about the process. The difference in speed between sensors 1 and 2 could be related to the longer path of the wave, if it travelled with a curved geometry as seen with BOS-method. However, the resulting error in velocity due to curvature was a factor ten smaller than the actual measured difference. This illustrated the assumption that the edge of the wave lagged behind the center. One effect that explains this behavior is the whip effect described in [8], caused by the sheet metal clamping used.

Summary and Conclusion

In this paper a multi-sensor approach was introduced to electrohydraulic forming and proven as a concept for in-process pressure wave analysis. The following observations were summarized:

- Different sensor data were usable to describe the pressure wave along the pressure vessel.
- BOS-method directly delivered an insight to the pressure wave from curvature to velocity.
- The pressure wave velocity varied along the pressure vessel with velocities up to 1800 m/s.
- Pressure sensor data could be related to near-field behavior detecting the lowest velocities.
- The change in shockwave velocity with loading energy and wire material was related to the change of sound velocity of compressed water.

As a conclusion, the energy transmission could be described by near-field effects like the wire explosion and resulting time delay and far-field effects like the transient pressure wave front with a pressure amplitude and geometry. The energy transmission ends in the impulse transfer and reaction of the sheet metal after been reached by the pressure wave.

Acknowledgments

The authors gratefully acknowledge the support by the German Research Foundation DFG for the project “Wirkmedienbasierte Impulsumformung von Kanalstrukturen”. This research was funded by the DFG (German Research Foundation), grant number 529030284.

References

[1] Q. J. Zhao et al.„„Study of micro electro-magnetic bulging on a stainless-steel foil“, Manufacturing Review, 2, 2015.

[2] E. Cantergiani et al., „Example of two industrial Electro-hydraulic forming applications highlighting the advantages of high strain rates”, Conference: NEBU NEHY, 2018.

[3] R. Han, „Electrical Explosion in a Medium: Plasmas, Shock Waves, and Applications”, in: T. Shao and C. Zhang (eds.), Pulsed Discharge Plasmas, Springer Series in Plasma Sc. and Tech.

[4] S. Efimov et al., „Addressing the efficiency of the energy transfer to the water flow by underwater electrical wire explosion”. Journal of Applied Physics, 106 (7).

[5] Y. Tagawa Y et al. „On pressure impulse of a laser-induced underwater shock wave“, Journal of Fluid Mechanics. 2016.

[6] H. Shu et al., „Measurement of the sound velocity of shock compressed water”. Sci R. 11, 2021.

[7] I. Eguia et al., „Pressure Field Stabilisation in High-Voltage Underwater Pulsed Metal Forming Using Wire-Initiated Discharges, Key Engineering Materials Vol. 473, 2011.

[8] L. Langstädtler and C. Schenck, „Strain rates in electrohydraulic forming of thin stainless-steel sheet metals”, International Conference on High-Speed Forming, Dortmund, 2025.

[9] A.V. Mamutov et al., „Modeling of electrohydraulic forming of sheet metal parts”, JMPT, 2015.

[10] JoshtheEngineer (2021): BOS matlab script. online via github.com

The publication of this article was funded by the University of Bremen